

Three-dimensional photolithographic patterning of multiple bioactive ligands in poly(ethylene glycol) hydrogels†

Joseph C. Hoffmann and Jennifer L. West*

Received 22nd March 2010, Accepted 4th June 2010

DOI: 10.1039/c0sm00140f

The biomaterials community is faced with the challenge of imitating a vastly complex, physiological tissue environment. While cellular systems towards this end have been traditionally studied in two dimensions (2D), most cells require three-dimensional (3D) cues to produce a physiologically relevant response. Two-photon absorption laser scanning lithography (TPA-LSL) may be applied to photosensitive hydrogel systems to engineer heterogeneous, 3D microenvironments consisting of precisely patterned bioactive signals. In this work, we have developed new operating parameters and system capabilities for TPA-LSL through the patterning of fluorescently labeled monoacrylate PEG-RGDS within PEG-DA hydrogels. Specifically, we have demonstrated a flexible pattern size range, with features ranging from 1 μm to nearly 1 mm. We have also shown patterns of differing concentrations of the cell adhesive ligand RGDS and correlated observed RGDS fluorescence with laser scan speed and intensity. Finally, we have micropatterned multiple, unique bioactive ligands into distinct, 3D forms within a single hydrogel. The results presented here have significantly developed the capabilities of the TPA-LSL micropatterning technique to allow for the fabrication of heterogeneous, 3D cellular microenvironments, which should prove highly useful for future biomimetic applications.

Introduction

A tremendous amount of research has focused on the design of complex biomaterials to recreate a physiological tissue environment, with potential applications ranging from the development of pharmaceutical assays and diagnostics to the production of drug delivery devices and tissue engineered therapeutics.¹ Much of this work has focused on the study of cell–biomaterial interactions in two dimensions (2D); however, recent findings have shown that nearly all cell types require three-dimensional (3D) cues to produce a physiologically relevant response.² In order to mimic physiological tissue structures, it is of critical importance to design and fabricate 3D microenvironments in which bioactive signals may be presented in a precisely controlled manner.

Recently, researchers have utilized hydrogels as a useful medium to engineer a 3D biological microarchitecture, taking advantage of their tunable physical and chemical properties.^{3,4} Poly(ethylene glycol) (PEG) hydrogels, in particular, have been used extensively due to their well established biocompatibility, inherent resistance to protein absorption, and ease of physical and chemical modification.^{5,6} More specifically, PEG macromers modified with an acrylate group at each terminus will rapidly polymerize upon exposure to light in the presence of an appropriate photoinitiator. These PEG-based hydrogels act as a “blank slate” into which biochemical cues may be incorporated, thus allowing for the introduction of bio-functionalized patterns *via* controlled light exposure.^{7,8}

In parallel with the development of versatile hydrogel materials, a variety of microfabrication techniques have emerged with the goal of transforming these materials into structures that offer a 3D microenvironment. In particular, 3D printing, soft lithography, microfluidics and photolithography have been utilized with increasing success to fabricate biomaterials with designed 3D features on the microscale.⁹ However, these techniques generally employ a sequential layering method to create microstructures with desired axial depths and at times suffer from lack of fidelity and chemical control in the axial dimension.¹⁰

The use of a two-photon excitation process to directly modify preformed, photosensitive hydrogel scaffolds offers a straightforward alternative for the fabrication of 3D microenvironments. Utilizing the simultaneous absorption of two photons from a high frequency pulsed laser, excitation volumes may be effectively limited to a minute focal volume.¹¹ Two-photon absorption laser scanning lithography (TPA-LSL) in photosensitive materials takes advantage of this phenomenon by confining the photo-reactive processes to focused, 3D micro-volumes, leaving all other points along the laser's optical path unaltered.¹² Previously, TPA-LSL has been applied to poly(ethylene glycol)-diacrylate (PEG-DA) hydrogels, among other materials, yielding complex 3D patterns and gradients of biomolecules.^{8,12–17}

Despite this significant advance in 3D microenvironment fabrication technology, relatively little progress has been made towards the application of TPA-LSL to tissue engineering and fundamental cellular biology. The growth of TPA-LSL applications has instead been stunted by a lack of development of its key operating parameters and system capabilities. In this work, we have characterized and expanded upon several critical aspects of TPA-LSL through the micropatterning of fluorescently labeled monoacrylate PEG-RGDS peptide in PEG-DA hydrogels. Specifically, we have demonstrated the ability to pattern

Department of Bioengineering, MS-142, Rice University, 6100 Main Street, Houston, Texas, 77005, USA. E-mail: jwest@rice.edu; Fax: +1 713-348-5877; Tel: +1 713-348-5955

† This paper is part of a joint *Soft Matter* and *Journal of Materials Chemistry* themed issue on Tissue Engineering. Guest editors: Molly Stevens and Ali Khademhosseini.

RGDS over several different size ranges, and probed the lateral and axial resolution limits of the TPA-LSL technique. Further, we have characterized the effect of laser scan speed and intensity on the concentration of patterned RGDS, and demonstrated the versatility of TPA-LSL by fabricating micropatterns of varying 3D shape. We have also shown patterns of multiple, spatially overlapping acrylate-PEG-RGDS moieties, to serve as a proof of concept for fabricating a complex, heterogeneous cellular microenvironment. Finally, we report the micropatterning of two distinct, fibronectin derived peptides (RGDS and CS-1) within a collagenase degradable PEG-DA hydrogel to demonstrate a seamless transition towards the patterning of different types of adhesive ligands and growth factors within photosensitive, biodegradable materials. These results demonstrate the versatility and effectiveness of TPA-LSL as a technique to fabricate complex biological landscapes at the microscale and should serve as a solid foundation upon which a variety of biomimetic technologies may be built.

Materials and methods

Poly(ethylene glycol)-diacrylate (PEG-DA) synthesis and purification

Dry poly(ethylene glycol) (PEG, 3400 Da; Fluka) was reacted with acryloyl chloride (Sigma) at a 1 : 4 molar ratio in anhydrous dichloromethane (DCM; Sigma) with triethyl amine (TEA; Sigma) at a 1 : 2 molar ratio (PEG : TEA). The reaction was stirred overnight under argon and washed with 2 M K_2CO_3 to remove chloride salt *via* phase separation. The PEG-DA containing organic phase was dried using anhydrous $MgSO_4$, filtered, and precipitated in diethyl ether. The final PEG-DA product was filtered, dried overnight under vacuum, and characterized by 1H NMR.

Synthesis of monoacrylate PEG-peptides and degradable PEG-DA hydrogels

Acrylate-poly(ethylene glycol)-succinimidyl carboxymethyl (PEG-SCM; Laysan) dissolved in dimethyl sulfoxide (DMSO; Cambridge Isotope Laboratories) was slowly dripped into a solution of cell-adhesive RGDS peptide (American Peptide) with *N,N*-diisopropylethylamine (DIPEA; Sigma) in DMSO so that the final molar ratios were 1 : 1.2 (PEG-SCM : RGDS) and 1 : 2 (PEG-SCM : DIPEA). The resulting solution was rapidly mixed under argon for 24 h, cooled on ice and mixed with Millipore water. The monoacrylate-PEG-RGDS product was dialyzed against Millipore water for 12 h using a 3500 MWCO regenerated cellulose membrane (Spectrum Laboratories) and lyophilized to dryness. Similarly, the peptide QILDVPST (abbreviated CS-1, American Peptide) was reacted with PEG-SCM in exactly the same manner to produce acrylate-PEG-CS-1. Degradable PEG-DA hydrogels were synthesized, as reported previously,¹⁸ through the incorporation of a collagenase-sensitive peptide linker into the backbone of the base PEG-DA polymer chains. Specifically, the peptide GGGPQGIWGQGK (abbreviated PQ) was synthesized *via* solid phase peptide synthesis with standard F-Moc chemistry using an Apex396 peptide synthesizer (Aapptec, Louisville, KY, USA). Successful peptide synthesis was confirmed using matrix assisted laser desorption ionization

time of flight mass spectrometry (MALDI-ToF; Bruker Daltonics, Billerica, MA, USA). The purified peptide was reacted with PEG-SCM *via* a procedure similar to monoacrylate PEG-peptide conjugation, with the final molar ratios of 1 : 2.1 (PEG-SCM : PQ) and 1 : 2 (PEG-SCM : DIPEA). Monoacrylate-PEG-peptide and collagenase degradable PEG-DA were both characterized *via* gel permeation chromatography (GPC; Polymer laboratories, Amherst, MA, USA) with detectors for UV-vis and evaporative light scattering.

Fluorescent tagging of monoacrylate PEG-peptides

Purified monoacrylate PEG-RGDS in 0.1 M sodium bicarbonate (pH 9) was further reacted with Alexa Fluor® 488 carboxylic acid 2,3,5,6-tetrafluorophenyl ester (AF488-TFP; Invitrogen) in dimethylformamide at a 1 : 10 molar ratio (acrylate-PEG-RGDS : AF488-TFP). This reaction was rapidly mixed for 2 h and dialyzed for 12 h against Millipore water with a 3500 MWCO regenerated cellulose membrane. The resulting monoacrylate-PEG-RGDS-Alexa Fluor® 488 was lyophilized to dryness and stored at -20 °C. This reaction was carried out in the same manner with Alexa Fluor® 532 carboxylic acid succinimidyl ester (AF532-SE; Invitrogen), or Alexa Fluor® 633 carboxylic acid succinimidyl ester (AF633-SE; Invitrogen) dissolved in 0.1 M sodium bicarbonate buffer (pH 8.3) to form monoacrylate-PEG-RGDS-Alexa Fluor® 532 and monoacrylate-PEG-RGDS-Alexa Fluor® 633, respectively. A similar procedure was followed to fluorescently label monoacrylate-PEG-CS-1.

PEG-DA hydrogel fabrication

A glass coverslip was piranha etched, exposed to Millipore water, and incubated with 85 mM 3-(trimethoxysilyl)propyl methacrylate (Fluka) in ethanol (pH 4.5) to introduce surface acrylate groups to the glass.¹⁵ Hydrogel molds were constructed by securing a 0.5 mm thick poly(tetrafluoroethylene) (PTFE) spacer between an acrylated coverslip and a glass slide. A prepolymer solution of 10% (w/v) PEG-DA in HBS with $10 \mu L mL^{-1}$ of $300 mg mL^{-1}$ 2,2-dimethoxy-2-phenylacetophenone (DMPAP) in *N*-vinyl pyrrolidone (NVP) was prepared. The prepolymer solution was injected into the mold and exposed to long wavelength ultraviolet light (B-200SP UV lamp, UVP, 365 nm, $10 mW cm^{-2}$) for 45 s, forming a crosslinked and immobilized hydrogel on the acrylated glass coverslip. Immobilized hydrogels were soaked in filtered HBS until further use. The degradable hydrogels were fabricated *via* the same procedure using 10% (w/v) collagenase degradable PEG-DA.

Design of 3D patterns of fluorescent monoacrylate PEG-RGDS

Patterns of desired dimensionality and concentration were specified using the region of interest (ROI) function in the LSM software (Carl Zeiss Inc) by selecting the laser intensity, laser scan speed, microscope objective, and Z plane focus. Specifically, a 10× Plan-Apochromat objective lens (NA 0.4), a 20× Plan-Apochromat objective lens (NA 0.75) and a 63× Plan-Apochromat objective lens (NA 1.4) were utilized to create patterns of varying size. To tune the concentration of crosslinked fluorescent monoacrylate PEG-RGDS molecules, scan speeds of

204 μs per pixel, 102 μs per pixel and 51 μs per pixel were utilized. Additionally, pattern concentrations were also varied using laser intensities of 25 $\text{mW } \mu\text{m}^{-2}$, 21 $\text{mW } \mu\text{m}^{-2}$, and 17 $\text{mW } \mu\text{m}^{-2}$. Unless otherwise specified, patterns were generally fabricated using the 20 \times objective with a scan speed of 204 μs per pixel, and a laser intensity of 25 $\text{mW } \mu\text{m}^{-2}$. To fabricate continuous patterns in the Z direction, the focus was adjusted upwards 3 μm in between subsequent scans. Patterns shown were created using 3–5 scans each separated by 3 μm , unless otherwise specified. To create patterns of varying 3D shapes, the designed ROI was modified for differing Z planes.

Patterning fluorescent acrylate-PEG-RGDS using two-photon absorption laser scanning lithography

The TPA-LSL methodology for fabricating 3D patterns of fluorescent monoacrylate-PEG-RGDS in PEG-DA hydrogels is outlined in Fig. 1. A crosslinked, immobilized PEG-DA hydrogel was incubated in a solution of monoacrylate-PEG-RGDS-Alexa Fluor® 488 (5–10 nmol mL^{-1}) in HBS with 10 $\mu\text{L mL}^{-1}$ of 300 mg mL^{-1} DMAP in NVP for 30 min under gentle rocking conditions. The hydrogel was positioned on the stage of an LSM 510 META NLO confocal microscope (Carl Zeiss Inc.). A titanium/sapphire laser tuned to 720 nm was scanned across a pre-designed ROI to initiate crosslinking of free acrylate groups in desired, free-form 3D patterns. After patterning, the hydrogel was washed extensively with HBS under gentle rocking for 48 h to remove unbound fluorescent monoacrylate-PEG-RGDS and photoinitiator. The resulting patterns were imaged using traditional confocal microscopy and projected and analyzed using ImageJ (NIH Bethesda, MD). A background subtraction was applied to reduce the auto-fluorescence of the PEG-DA hydrogel.

To pattern multiple fluorescent variants of RGDS, an immobilized PEG-DA hydrogel was patterned with PEG-RGDS-Alexa Fluor® 488 as described above. After washing, the hydrogel was incubated in a solution of monoacrylate-PEG-RGDS-Alexa Fluor® 532 (5–10 nmol mL^{-1}) in HBS with 10 $\mu\text{L mL}^{-1}$ of 300 mg mL^{-1} DMAP in NVP for 30 min with gentle rocking. Patterns of PEG-RGDS-Alexa Fluor® 532 were created as before through the scanning of the 720 nm laser across designed regions of interest. The unbound monoacrylate PEG-RGDS-Alexa Fluor® 532 and photoinitiator were washed out for 48 h, allowing for the visualization of both fluorescent PEG-RGDS patterns *via* the confocal microscope. This technique was repeated with the incubation of monoacrylate-PEG-RGDS-Alexa Fluor® 633, so that after laser scanning and washing, 3 different types of patterned fluorescent PEG-RGDS in close proximity to each other were visualized within a single PEG-DA hydrogel. In these studies, RGDS with the 3 fluorophores was simply used as a model peptide to demonstrate the feasibility of repetitive patterning of multiple moieties. The exact same procedure was later utilized to pattern both PEG-RGDS-Alexa Fluor® 488 and PEG-CS-1-Alexa Fluor® 633 within a degradable PEG-DA hydrogel.

Results

Fabrication of fluorescent RGDS patterns of varying size

To establish the versatility of TPA-LSL as a biomolecular patterning strategy, ROIs were designed to demonstrate the capability of the technique to create precise, fluorescent RGDS patterns over a large size range. Patterns of fluorescent RGDS were created within PEG-DA hydrogels utilizing the different fields of

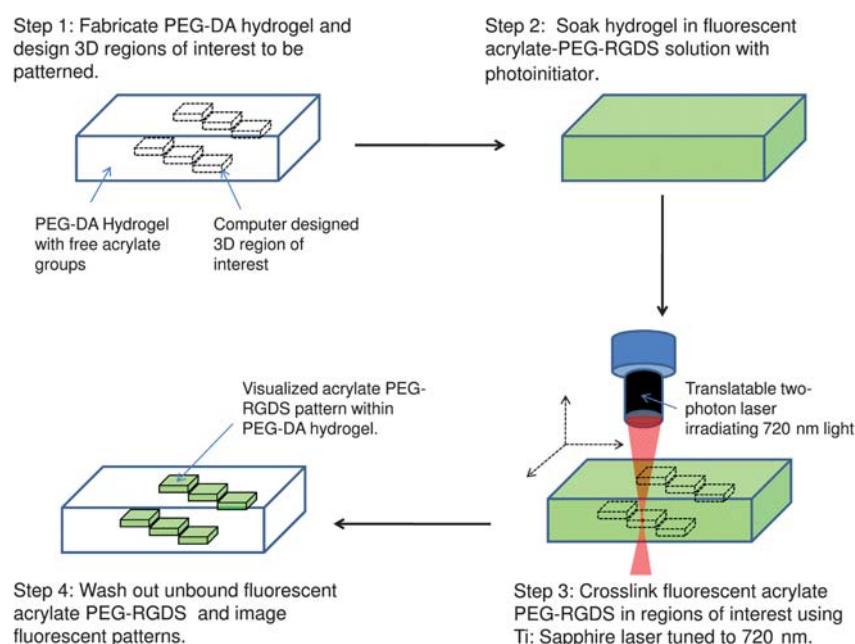


Fig. 1 TPA-LSL methodology. A PEG-DA hydrogel was fabricated and 3D ROIs were designed using LSM software. Fluorescent monoacrylate PEG-RGDS solution with photoinitiator was soaked into the PEGDA hydrogel, and a Ti:Sapphire laser tuned to 720 nm was used to crosslink the fluorescent PEG-RGDS moieties in desired free form 3D patterns. The PEG-DA gels were washed thoroughly and imaged.

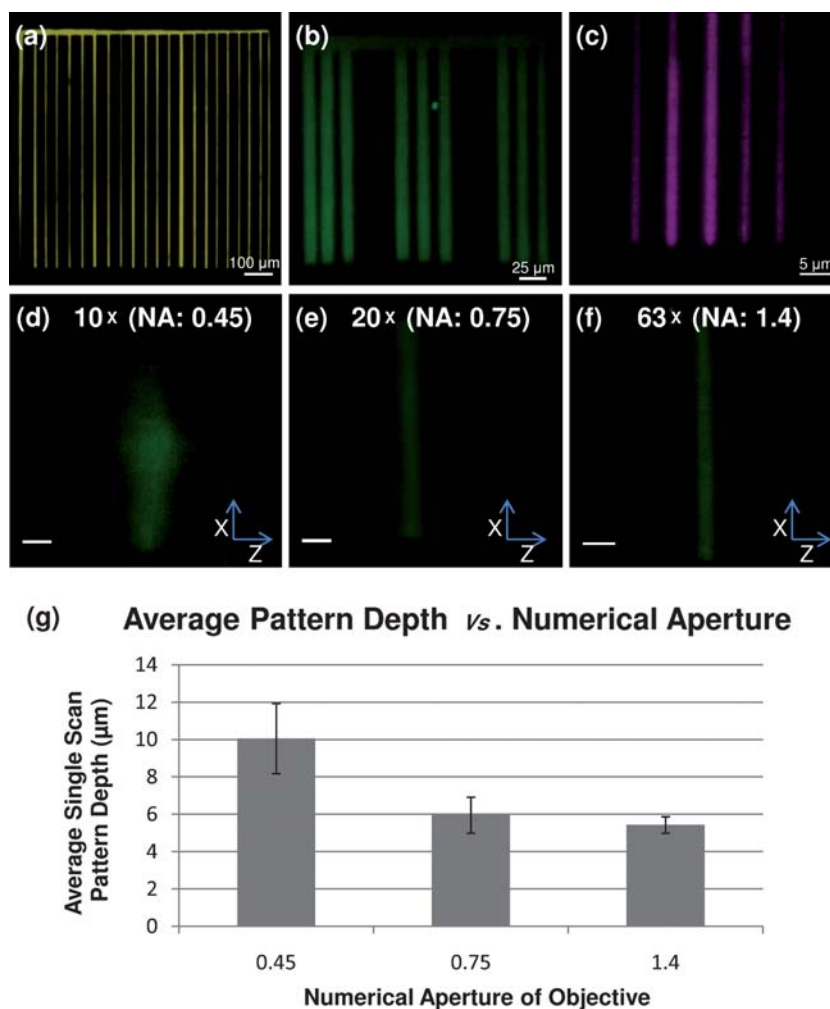


Fig. 2 (a–c) Confocal fluorescent images of patterned fluorescent PEG-RGDS within PEG-DA hydrogels. (a) PEG-RGDS-Alexa Fluor®633 pattern fabricated using a 10X objective. Scale bar = 100 μm . (b) PEG-RGDS-Alexa Fluor®488 pattern fabricated using a 20X objective. Scale bar = 25 μm . (c) PEG-RGDS-Alexa Fluor®532 pattern fabricated using a 63X objective. Scale bar = 5 μm . (d–e). 3D projections of the axial resolution of patterned PEG-RGDS-Alexa Fluor®488 within a PEG-DA hydrogel resulting from a single laser scan at one focal depth. Patterns created using (d) 10X objective with NA 0.45. (e) 20X objective with NA 0.75. (f) 63X objective with NA 1.4. Scale bars = 10 μm . (g) Plot of average pattern axial resolution from a single laser scan at a particular focal depth from objectives with a wide range of numerical apertures.

view of the 10 \times , 20 \times and 63 \times objectives to scan the 720 nm light over different ROIs. The results, as seen in Fig. 2, show patterns that vary in size over nearly 3 orders of magnitude. A pattern created with the 10 \times objective (Fig. 2a) spans 950 μm in both lateral directions. Additionally, the thin bars in this pattern indicate a high resolution on the order of 5–10 μm with the 10 \times objective, demonstrating the ability to create patterns spanning nearly 1 mm across the hydrogel with micron range control of feature size. To probe the lateral resolution limit of TPA-LSL, a pattern was created using the 63 \times objective (Fig. 2c). This pattern showed well defined features 1–2 μm in width, demonstrating the ability to pattern peptides within PEG-DA hydrogels in a size range highly relevant to the cellular microenvironment.

Axial resolution of fluorescent RGDS patterning in PEG-DA hydrogels

Patterns of fluorescent RGDS were also created within PEG-DA hydrogels to probe the axial resolution of TPA-LSL. This test was

performed for an array of microscope objectives with different numerical apertures. Simple ROIs were designed and a single scan of the 720 nm laser across the ROI was performed. This single scan resulted in crosslinking of fluorescent monoacrylate PEG-RGDS in a particular focal plane, and thus, all crosslinking that occurred represented the axial resolution limit. This resolution testing procedure was carried out for the 10 \times , 20 \times , and 63 \times microscope objectives with numerical apertures (NA) of 0.4, 0.75, and 1.4. Resulting patterns were imaged with a confocal microscope, and 3D projections (Fig. 2d–f) were constructed to measure the smallest possible thickness of fluorescent RGDS patterns within PEG-DA hydrogels. Patterns fabricated from the 0.4 NA objective resulted in an axial resolution of approximately 10 μm , while the 0.75 NA and 1.4 NA objectives resulted in approximate axial resolution limits of 5.9 μm and 5.4 μm respectively (Fig. 2g). It should be noted that patterns created with larger numerical aperture objectives not only have higher axial resolution, but also show a sharper contrast between patterned and non-patterned regions in the axial dimension.

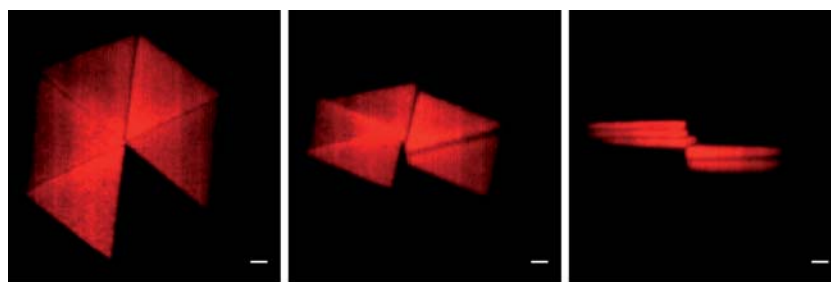


Fig. 3 3D projections of patterned PEG-RGDS-Alexa Fluor@488 within a PEG-DA hydrogel. Images shown depict a single pattern viewed with an increasing angle of rotation. From left to right pattern is rotated 0° , 45° , and 90° away from the viewer. All Scale bars = $10\ \mu\text{m}$.

Demonstration of the three dimensionality of TPA-LSL patterns

To demonstrate the ability to pattern biomolecules such as RGDS into distinct, 3D forms, fluorescent RGDS was cross-linked into a spiral staircase pattern within a PEG-DA hydrogel (Fig. 3). Specifically, 5 individual steps of the staircase were designed, each using a particular ROI. Each step was fabricated *via* 3 sequential scans of the 720 nm laser across the ROI, with each scan separated by a $3\ \mu\text{m}$ increment in the axial direction. The axial resolution of TPA-LSL within PEG-DA hydrogels is such that 3 scans separated by $3\ \mu\text{m}$ form a continuously patterned region. Between each step of the staircase, the focus was adjusted $6\ \mu\text{m}$ axially and the new ROI was selected so that upon imaging with a confocal microscope, a projection was generated that allowed for the visualization of the three dimensionality of the fluorescent RGDS staircase pattern within the PEG-DA hydrogel (Fig. 3). It follows that TPA-LSL may be further applied to confine biomolecules such as RGDS, or other peptides or proteins, to any desired 3D volume within a PEG-DA hydrogel network.

Controlling fluorescent RGDS concentration with laser scan speed and intensity

The LSM software allowed for increased versatility of TPA-LSL in that the laser scan speed and laser intensity may be precisely specified to control the concentration of crosslinked RGDS. Patterns were created in which distinct ROIs were defined and each one was patterned with a different laser scan speed. Three different Y-shaped ROIs were specified and patterned *via* the 720 nm laser at 3 distinct scan speeds with constant laser intensity. Specifically, the innermost region was patterned using a scan speed of $204\ \mu\text{s}$ per pixel, the middle region was patterned with a scan speed of $102\ \mu\text{s}$ per pixel and the outermost region was patterned with a scan speed of $51\ \mu\text{s}$ per pixel. A fluorescence intensity profile of this pattern (Fig. 4a) shows 3 distinct regions of fluorescence intensity in which longer laser dwell times on each pixel correlated with higher fluorescence intensity values. As the fluorescence intensity relates directly to the crosslinking of fluorescent RGDS molecules, TPA-LSL provides a clear control of relative RGDS concentration within PEG-DA hydrogels. The degree of crosslinking of fluorescent RGDS may also be modified *via* laser intensity control. Fig. 4b shows an array of 9 distinct square patterns of fluorescent RGDS within a PEG-DA hydrogel, each of which was fabricated *via* the selection of a unique combination of laser intensity and scan speed. Laser intensities

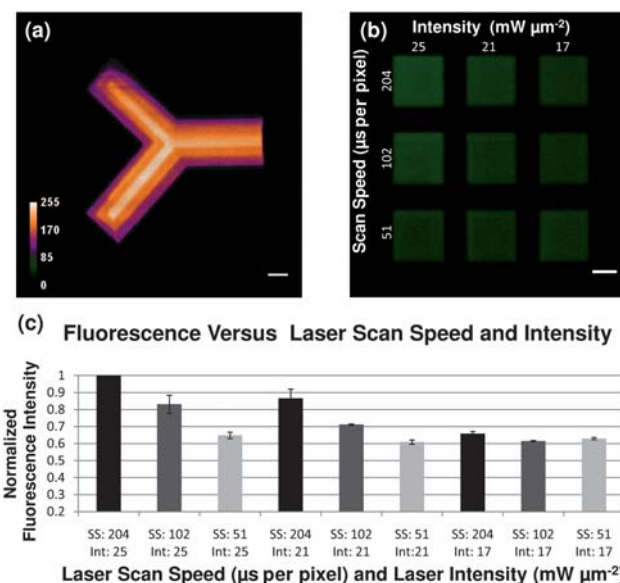


Fig. 4 (a) Fluorescence intensity profile of patterned monoacrylate-PEG-RGDS-Alexa Fluor@488 with varying scan speeds. Outside pattern $204\ \mu\text{s}/\text{pixel}$, middle pattern $102\ \mu\text{s}/\text{pixel}$, and inside pattern $51\ \mu\text{s}/\text{pixel}$. Scale bar = $25\ \mu\text{m}$. (b) Confocal fluorescence image of patterned monoacrylate-PEG-RGDS-Alexa Fluor@488 with varying scan speeds and laser intensities. Scale bar = $25\ \mu\text{m}$. (c) Plot of the effects of scan speed and laser intensity when crosslinking on observed normalized fluorescence of imaged pattern. Pattern with highest observed fluorescence normalized to 1.

utilized were $25\ \text{mW}\ \mu\text{m}^{-2}$, $21\ \text{mW}\ \mu\text{m}^{-2}$, and $17\ \text{mW}\ \mu\text{m}^{-2}$ while scan speeds were varied as described above. Fluorescence intensity measurements were taken for each patterned region and normalized to the pattern with the highest intensity (Fig. 4c). It was shown that both laser intensity and scan speed have a direct correlation to patterned fluorescent RGDS, as fluorescence intensity values declined by up to 40 percent for decreasing scan speeds and decreasing laser intensities. The combination of laser intensity and scan speed may be referred to together as the applied energy over a given area or laser fluence. The designation of laser fluence specifies the amount of energy in the excitation focal volume, and therefore, positively correlates with the amount of crosslinking of acrylate-PEG-RGDS. Accordingly, these data relating laser scan speed and laser intensity to the fluorescence of RGDS (Fig. 4c) may be utilized to pattern desired concentrations of biomolecules within hydrogel networks using TPA-LSL.

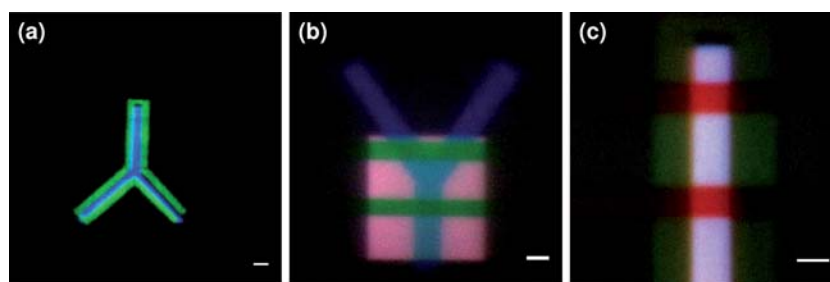


Fig. 5 Confocal fluorescent images of patterns of multiple types of fluorescent monoacrylate PEG-RGDS within a PEG-DA hydrogel. (a) PEG-RGDS-Alexa Fluor®488 pattern juxtaposed to PEG-RGDS-Alexa Fluor®633 pattern. Scale bar = 25 μm . (b–c) PEG-RGDS-Alexa Fluor®488 pattern overlapping patterns of PEG-RGDS-Alexa Fluor®633 and PEG-RGDS-Alexa Fluor®532. Scale bars = 10 μm .

Patterning multiple fluorescent RGDS variants

To show the feasibility of patterning multiple biomolecules into distinct 3D forms within a PEG-DA hydrogel network, several variants of fluorescent RGDS were utilized. PEG-RGDS-Alexa Fluor® 488 was first allowed to diffuse into PEG-DA hydrogels and crosslinked into simple patterns *via* 720 nm light exposure across designed ROIs. Next, PEG-RGDS-Alexa Fluor® 532 was allowed to diffuse into the gel, and a ROI juxtaposed to the patterned PEG-RGDS-Alexa Fluor® 488 was designed. After irradiation, the two different versions of fluorescent RGDS were observed side by side in a single PEG-DA hydrogel (Fig. 5a). The versatility of TPA-LSL was further demonstrated with the conjugation of a third fluorescent RGDS moiety, PEG-RGDS-Alexa Fluor® 633 within the hydrogel. The 3 different varieties of PEG-RGDS were patterned in an overlapping manner so that there existed areas in which all 3 ligands were clearly present (Fig. 5b and c). These fluorescent RGDS variants may also be patterned in a way that more explicitly demonstrates the inherent three-dimensionality of the TPA-LSL strategy. To do this, each

fluorescent RGDS variant was crosslinked into the gel at a unique axial depth. By changing the design of the ROI for each fluorescent RGDS variant, complex, 3D patterns were created in PEG-DA hydrogels utilizing multiple different ligands. Fig. 6 shows two such multi-ligand, 3D patterns after confocal imaging.

Patterning RGDS and CS-1 peptide within a collagenase degradable hydrogel

To show the feasibility of fabricating a truly heterogeneous cellular microenvironment, two distinct, fibronectin derived peptides, namely RGDS and CS-1, were patterned within a degradable PEG-DA hydrogel. Specifically, the peptide GGGPQGIWGQGK (abbreviated as PQ) was synthesized and incorporated into PEG-DA hydrogels to render them degradable to cells secreting collagenase. PEG-RGDS-488 and PEG-CS-1-Alexa Fluor® 633 were patterned into the degradable PEG gels in a subsequent manner. In Fig. 7, 3 distinct patterns of RGDS (green) and CS-1 (blue) within a degradable PEG-DA hydrogel

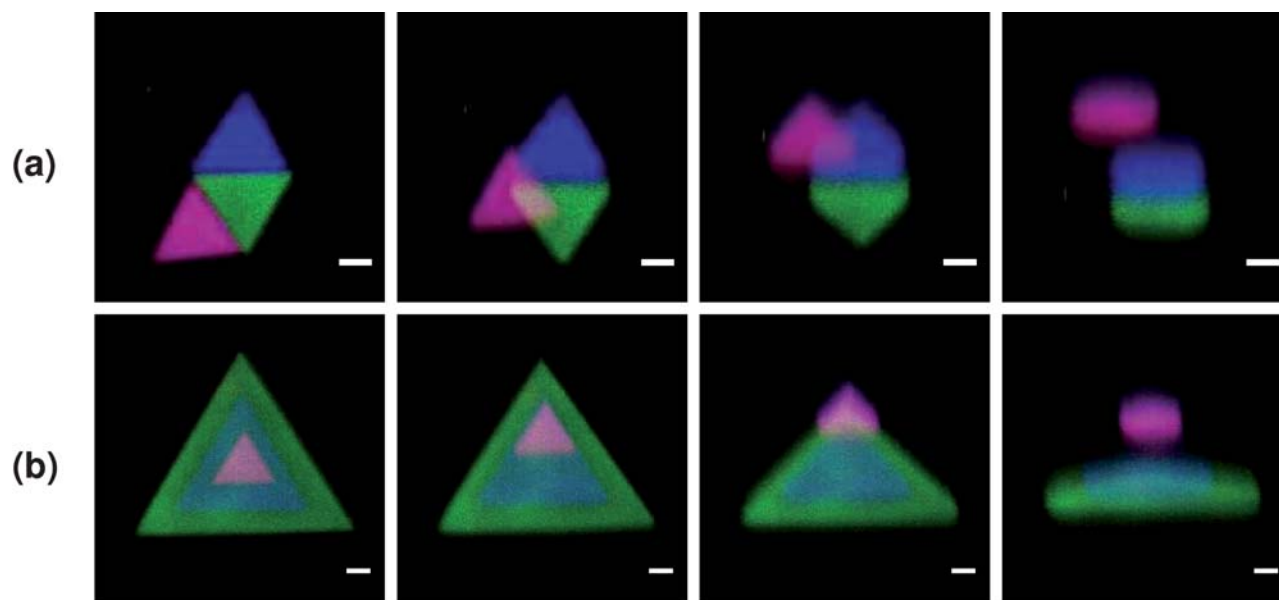


Fig. 6 (a–b) 3D projections of patterned PEG-RGDS-Alexa Fluor®488, PEG-RGDS-Alexa Fluor®633 and PEG-RGDS-Alexa Fluor®532. Images shown depict a single pattern viewed with an increasing angle of rotation. From left to right pattern is rotated 0°, 30°, 60°, and 90° away from the viewer. All Scale bars = 25 μm .

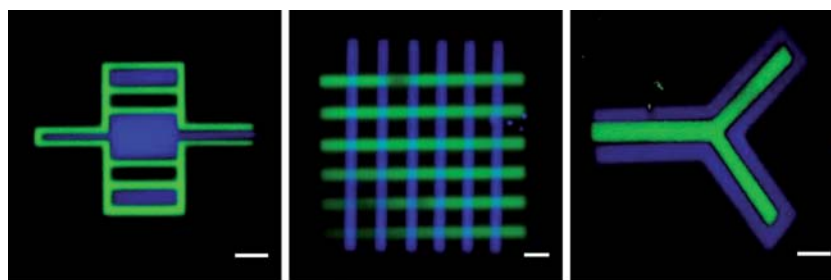


Fig. 7 Confocal fluorescent images of patterns of PEG-RGDS- Alexa Fluor@488 (green) and PEG-CS1- Alexa Fluor@633 within a collagenase degradable PEG-DA hydrogel. All Scale bars = 25 μm .

were imaged *via* confocal microscopy. Through similar patterning of multiple bioactive adhesive ligands and growth factors within a single degradable hydrogel, TPA-LSL may be utilized to design and engineer a variety of heterogeneous, 3D microenvironments within photosensitive, biodegradable materials.

Discussion

The development of TPA-LSL as a 3D microfabrication methodology has great potential to impact the field of bioengineering and biomedicine. Already, two-photon excitation technology has been utilized to pattern biomolecules within preformed photosensitive hydrogels.^{8,12–17} In a few of these cases, a 3D biochemical cue has been presented to cells incorporated within the patterned material. For example, work by Hahn *et al.*⁸ showed that cell migration could be restricted to a 3D, patterned area of RGDS. Similarly, Lee *et al.*¹² demonstrated direct guidance of fibroblast migration *via* 3D RGDS channels within degradable PEG-based hydrogels. Further, Seidlits *et al.* have shown guidance of dorsal root ganglion cells (DRGs) and hippocampal neural progenitor cells (NPCs) along 3D paths created *via* attachment of adhesive ligands to free-form, 3D protein structures created *via* two-photon initiated crosslinking.¹⁷ While these works demonstrate the feasibility and promise of guiding cell behavior in hydrogels using a single, 3D patterned biochemical cue, they have yet to utilize the potential of the TPA-LSL technique to guide cell motility and phenotype through the fabrication of complex physiological microenvironments. One reason for the low level of complexity thus far has been the lack of optimization of TPA-LSL parameters and system capabilities. The work presented here demonstrates the capability of two-photon laser patterning to create novel, cellular microenvironments consisting of multiple patterned biomolecules over a wide range of designated concentrations and 3D volumes.

Specifically, when designing a bioactive microenvironment, the maximum size range for pattern fabrication *via* TPA-LSL was shown to be dependent on the field of view (in the *XY* lateral dimension) and the focal distance (in the *Z* dimension) of the objective through which the 720 nm laser passed. The choice of objective also correlated with the lateral and axial resolutions of the TPA-LSL patterning technique as the numerical aperture of the objective lens is a determinate of the two-photon excitation volume. Fabricated patterns of biomolecules with minute feature size ($\sim 1 \mu\text{m}$) allowed for the creation of microenvironments highly relevant to individual cells. Future experiments will

explore how small groups of cells respond to multiple types of adhesive ligands and growth factors presented on a 3D micro-scale. Further, detailed patterning over distances of hundreds of micrometres with large field of view objectives will allow for the control of cellular migration and phenotype to form basic 3D tissue structures. Fabricating patterns in a juxtaposed manner using a “quilt-work” type strategy will allow for the creation of biomolecule patterns across even larger volumes on the size order of human tissues.

Controlling the concentration of biomolecules within hydrogels, as demonstrated above, will also be crucial to cellular control. For example, while 2D cell migration has been studied in great detail, only recently have investigators begun to quantify 3D cell motility in response to biochemical factor presentation.¹⁹ The adjustment of laser scan speeds and intensities in TPA-LSL will allow for the fabrication of 3D gradients of adhesive proteins and growth factors which can then be utilized to study the complex cellular migratory response. Additionally, nearly all cell types respond differently to bioactive factors at unique concentrations, and the specification of the total amount of growth factor presentation to cells will allow for precise phenotypic control.

Perhaps even more essential to understanding complex cellular processes and recapitulating the *in vivo* cellular environment is the ability to three dimensionally pattern multiple biomolecules of differing functionalities within a given biomaterial. The current work demonstrates the robust capability of TPA-LSL to accomplish this task as both the RGDS and the CS-1 peptides were patterned within a single cellular microenvironment. RGDS, an amino acid sequence originally derived from the central cell binding domain of fibronectin, and CS1, an amino acid sequence derived from the alternatively spliced type 3 connecting segment of fibronectin,²⁰ have both been utilized extensively to study cell behavior on a variety of 2D substrates. The patterning of these two peptides (as well as many other known adhesion proteins and peptides) into a degradable hydrogel will allow for the elucidation of novel relationships between adhesion sites and cell surface integrins with regard to cell proliferation and motility in 3D.

Additionally, there have been many reported cases where multiple bioactive factors work synergistically to produce a dramatic overall effect on cells. For example, the simultaneous surface presentation of fibrinogen and vascular endothelial growth factor (VEGF) gradients to endothelial cells has resulted in a four-fold increase in cell migration along the gradient compared with fibrinogen alone.²¹ Further, the combination of

fibroblast growth factor (FGF)-2 and platelet derived growth factor (PDGF)-BB have been shown to synergistically induce stable vascular networks in an ischemic hind limb model.²² The ability to pattern multiple growth factors, such as those listed above, into precise, 3D volumes will allow for the elucidation of novel synergetic relationships between biomolecules and allow for a high level of cellular phenotypic control. TPA-LSL will also provide a means to pattern juxtaposed biomolecules that attract and affect differing cell types, and thus, allow for the organization of cells into three dimensionally designed physiological microstructures.

Conclusion

Cells in their natural environment respond to a myriad of protein signals that are presented within a 3D matrix. The signals are presented with micrometre precision over a large array of sizes. The signals also vary greatly with respect to their concentration throughout complex 3D volumes. In this work, we demonstrate the capability of two-photon absorption laser scanning lithography (TPA-LSL) to allow for the creation of complex cellular micro-environments with precise control of all these factors. Specifically, we demonstrated the ability to fabricate patterns from 1 μm to nearly 1 mm in lateral size, and with an axial resolution of approximately 5 μm . We further showed the ability to pattern different concentrations of adhesive ligand RGDS based on modulation of laser scanning properties. Finally, we demonstrated the ability to engineer 3D patterns of different types of biomolecules, first *via* the use of different fluorescent variants of RGDS, and then through the micropatterning of both RGDS and CS-1 within a single biodegradable, photosensitive hydrogel. The development of these abilities has enhanced the value of TPA-LSL as a patterning technique and should lead the way towards the design and fabrication of heterogeneous, 3D cellular microenvironments for a variety of biomimetic applications.

Acknowledgements

This work was supported by NIH grant R01 EB005173 and NIH grant P20 EB007076.

References

- 1 R. Langer and D. A. Tirrell, Designing materials for biology and medicine, *Nature*, 2004, **428**, 487–492.
- 2 L. G. Griffith and M. A. Swartz, Capturing complex 3D tissue physiology *in vitro*, *Nat. Rev. Mol. Cell Biol.*, 2006, **7**, 211–224.
- 3 A. Khademhosseini and R. Langer, Microengineered hydrogels for tissue engineering, *Biomaterials*, 2007, **28**, 5087–5092.

- 4 B. V. Slaughter, S. S. Khurshid, O. Z. Fisher, A. Khademhosseini and N. A. Peppas, Hydrogels in regenerative medicine, *Adv. Mater.*, 2009, **21**, 3307–3329.
- 5 K. T. Nguyen and J. L. West, Photopolymerizable hydrogels for tissue engineering applications, *Biomaterials*, 2002, **23**, 4307–4314.
- 6 J. L. Ifkovits and J. A. Burdick, Review: photopolymerizable and degradable biomaterials for tissue engineering applications, *Tissue Eng.*, 2007, **13**, 2369–2385.
- 7 M. S. Hahn, L. J. Taite, J. J. Moon, M. C. Rowland, K. A. Ruffino and J. L. West, Photolithographic patterning of polyethylene glycol hydrogels, *Biomaterials*, 2006, **27**, 2519–2524.
- 8 M. S. Hahn, J. S. Miller and J. L. West, Three-dimensional biochemical and biomechanical patterning of hydrogels for guiding cell behavior, *Adv. Mater.*, 2006, **18**, 2679–2684.
- 9 A. Khademhosseini, R. Langer, J. Borenstein and J. P. Vacanti, Microscale technologies for tissue engineering and biology, *Proc. Natl. Acad. Sci. U. S. A.*, 2006, **103**, 2480–2487.
- 10 Y. Luo and M. S. Shoichet, A photolabile hydrogel for guided three-dimensional cell growth and migration, *Nat. Mater.*, 2004, **3**, 249–253.
- 11 W. Denk, J. H. Strickler and W. Webb, Two-photon laser scanning fluorescence microscopy, *Science*, 1990, **248**, 73–76.
- 12 S.-H. Lee, J. J. Moon and J. L. West, Three-dimensional micropatterning of bioactive hydrogels *via* two-photon laser scanning photolithography for guided 3D cell migration, *Biomaterials*, 2008, **29**, 2962–2968.
- 13 R. G. Wylie and M. S. Shoichet, Two-photon micropatterning of amines within an agarose hydrogel, *J. Mater. Chem.*, 2008, **18**, 2716–2721.
- 14 C. A. DeForest, B. D. Polizzotti and K. S. Anseth, Sequential click reactions for synthesizing and patterning three-dimensional cell microenvironments, *Nat. Mater.*, 2009, **8**, 659–664.
- 15 V. L. Tsang, A. A. Chen, L. M. Cho, K. D. Jadin, R. L. Sah and S. DeLong, et al, Fabrication of 3D hepatic tissues by additive photopatterning of cellular hydrogels, *FASEB J.*, 2007, **21**, 790–801.
- 16 J. H. Wosnick and M. S. Shoichet, Three-dimensional chemical patterning of transparent hydrogels, *Chem. Mater.*, 2007, **20**, 55–60.
- 17 S. K. Seidlits, C. E. Schmidt and J. B. Shear, High-resolution patterning of hydrogels in three dimensions using direct-write photofabrication for cell guidance, *Adv. Funct. Mater.*, 2009, **19**, 3543–3551.
- 18 J. E. Leslie-Barbick, J. J. Moon and J. L. West, Covalently-immobilized vascular endothelial growth factor promotes endothelial cell tubulogenesis in poly(ethylene glycol) diacrylate hydrogels, *J. Biomater. Sci., Polym. Ed.*, 2009, **20**, 1763–1779.
- 19 M. H. Zaman, L. M. Trapani, A. Siemeski, D. MacKellar, H. Y. Gong and R. D. Kamm, et al, Migration of tumor cells in 3D matrices is governed by matrix stiffness along with cell-matrix adhesion and proteolysis, *Proc. Natl. Acad. Sci. U. S. A.*, 2006, **103**, 10889–10894.
- 20 A. Komoriya, L. J. Green, M. Mervic, S. S. Yamada, K. M. Yamada and M. J. Humphries, The minimal essential sequence for a major cell type-specific adhesion site (Cs1) within the alternatively spliced type-III connecting segment domain of fibronectin is leucine-aspartic acid-valine, *J. Biol. Chem.*, 1991, **266**, 15075–15079.
- 21 L. Y. Liu, B. D. Ratner, E. H. Sage and S. Y. Jiang, Endothelial cell migration on surface-density gradients of fibronectin, VEGF, or both proteins, *Langmuir*, 2007, **23**, 11168–11173.
- 22 R. H. Cao, E. Brakenhielm, R. Pawliuk, D. Wariaro, M. J. Post and E. Wahlberg, et al, Angiogenic synergism, vascular stability and improvement of hind-limb ischemia by a combination of PDGF-BB and FGF-2, *Nat. Med. (N. Y., NY, U. S.)*, 2003, **9**, 604–613.